

Enhancing the thermal performance of triple vacuum glazing with low-emittance coatings

Fang, Y. , Hyde, T.J. , Arya, F. , Hewitt, N. , Wang, R. and Dai, Y.

Post-print deposited in [Curve](#) April 2016

Original citation:

Fang, Y. , Hyde, T.J. , Arya, F. , Hewitt, N. , Wang, R. and Dai, Y. (2015) Enhancing the thermal performance of triple vacuum glazing with low-emittance coatings. Energy and Buildings, volume 97 (June): 186-195. DOI: 10.1016/j.enbuild.2015.04.006

<http://dx.doi.org/10.1016/j.enbuild.2015.04.006>

Elsevier

Creative Commons Attribution Non-Commercial No Derivatives License

Copyright © and Moral Rights are retained by the author(s) and/ or other copyright owners. A copy can be downloaded for personal non-commercial research or study, without prior permission or charge. This item cannot be reproduced or quoted extensively from without first obtaining permission in writing from the copyright holder(s). The content must not be changed in any way or sold commercially in any format or medium without the formal permission of the copyright holders.

CURVE is the Institutional Repository for Coventry University

<http://curve.coventry.ac.uk/open>

ENHANCING THE THERMAL PERFORMANCE OF TRIPLE VACUUM GLAZING WITH LOW-EMITTANCE COATINGS

Yueping Fang^{*1}, Trevor J. Hyde¹, Farid Arya¹, Neil Hewitt¹, Ruzhu Wang², Yanjun Dai²

¹School of the Built Environment, Ulster University, Newtownabbey BT37 0QB UK,

²School of mechanical engineering, Shanghai Jiao Tong University, Shanghai, 200240, China

ABSTRACT

The thermal performance of triple vacuum glazing (TVG) with one to four internal glass surfaces coated with a low-e (emittance) coating was simulated using a finite volume model. The simulated TVG comprises three, 4 mm thick glass panes with two vacuum gaps, sealed with indium metal and separated by an array of stainless steel pillars, 0.2 mm high, 0.3 mm diameter and spaced at 25 mm. The simulation results show that decreasing the emittance of the four low-e coatings from 0.18 to 0.03 reduces the heat transmission U-values at the centre-of-glazing area from $0.41 \text{ W.m}^{-2}.\text{K}^{-1}$ to $0.22 \text{ W.m}^{-2}.\text{K}^{-1}$ for a 0.4 m by 0.4 m TVG rebated by 10 mm within a solid wood frame. When using three low-e coatings in the TVG in a heating dominated climate, the vacuum gap with two low-e coatings should be set facing the warm environment, while the vacuum gap with one coating should face the cold environment. When using two low-e coatings with an emittance of 0.03, the U-values at the centre-of-glazing area with one coating in both vacuum gaps is $0.25 \text{ W.m}^{-2}.\text{K}^{-1}$; that with two coatings in the cold facing vacuum gap is $0.50 \text{ W.m}^{-2}.\text{K}^{-1}$ and that with two low-e coatings in the warm facing vacuum gap is $0.33 \text{ W.m}^{-2}.\text{K}^{-1}$. Thus setting one low-e coating in both vacuum gaps is better than setting two coatings in the same vacuum gap. The thermal performance of fabricated 0.4 m by 0.4 m TVGs with two and three low-e coatings were experimentally characterised and were found to be in very good agreement with simulation results.

KEY WORDS: Triple vacuum glazing, low-emittance coating, thermal performance, finite volume model

1. INTRODUCTION

The concept of vacuum glazing was first patented by Zoller [1]. Since the publishing of the patent nearly 90 years ago, there have been many further patents on vacuum glazing [2, 3]. However the first fabricated vacuum glazing was reported by a team at the University of Sydney in 1989 which used a solder glass with a melting point of 450°C to seal the periphery of the vacuum gap [4]. Since then a number of edge sealing techniques have been proposed such as a Spring Band Edge Seal [5], a novel solder glass sealing process [6] and an Alkali Silicate Edge Seal [7]. Collaborating with Baechli [8], the Fraunhofer Institute for Solar Energy Systems [9] developed an edge

^{*} Corresponding author. Tel: +44 28 90366808; fax: +44 2890368239. Email address: y.fang@ulster.ac.uk; fangyueping@hotmail.com (Y. Fang)

36 seal for vacuum glazing based on a sputtered metallic layer and a soldering technique, but this work has not been
37 published in a scientific journal. Recently, EverSealed Windows Inc. (US) [10, 11] and the German consortium
38 ProVIG [12] designed a vacuum glazing where a thin, flexible strip of metal is bonded to the glass using ultrasonic
39 welding or a soldering process. This flexible edge seal was designed to accommodate the differential thermal
40 expansion of the glass panes when subjected to a large temperature difference (e.g. 35 °C) between the indoor and
41 outdoor environments. A thermal transmission (U-value) of 0.5 W.m⁻².K⁻¹ for vacuum glazing using these
42 technologies has been achieved. However, such technologies are still in the development stage.

43 Using the method developed by the University of Sydney, samples up to 1 m by 1 m with a U-value of 0.80
44 W.m⁻².K⁻¹ in the centre-of-glazing area with a pillar diameter of 0.25 mm have been produced in the laboratory [13].
45 Due to the high fabrication temperature, many soft coatings and tempered glass cannot be used, since both will
46 degrade at this sealing temperature. The second fabrication method was developed by a team at Ulster University
47 [14, 15]. In this method, an indium based alloy with a melting temperature of less than 200 °C was used as the edge
48 sealant, making the use of a wide range of soft coatings and tempered glass possible. For 0.4 m by 0.4 m samples, a
49 U-value of 0.86 W.m⁻².K⁻¹ at the centre-of-glazing area with a pillar diameter of 0.4 mm has been achieved
50 experimentally [16].

51 It has been shown that when the vacuum pressure between the glass sheets is lower than 0.1 Pa, the heat
52 convection and conduction of gas can be ignored [13]. Both analytic and finite element models have proved that the
53 heat transfer in the centre-of-glazing depends on the heat conduction through the support pillar arrays and radiative
54 heat flow between the glass sheets. Infrared thermographs reveal a small variation in glass surface temperature that
55 occurs over the support pillars [17]. To further reduce heat transfer through the centre-of-glazing area, two possible
56 approaches could be considered. The first is to reduce the pillar diameter or increase the spacing, however beyond
57 certain limits, the glass will fracture. The minimum diameter is restricted by mechanical rules outlined by Collins
58 and Simko [13]. The second possible approach is to reduce radiative heat transfer by reducing the emittance of the
59 low-e coating. The lowest emittance of a soft low-e coating achieved so far is 0.02. When these approaches are at
60 limiting values, the principle way to further reduce the heat transmission of vacuum glazing is to add a second
61 vacuum gap by integrating a third glass sheet with a low-e coating. A team of Swiss Federal Laboratories for
62 Material Testing and Research has presented the viability of triple vacuum glazing (TVG) [18]. The mechanical
63 design constraints were investigated and a U-value of 0.2 W.m⁻².K⁻¹ in the centre-of-glazing area was predicted
64 when using an array of stainless steel pillars with a diameter of 0.3 mm and four low-e coatings within two vacuum
65 gaps. Based on the finite volume model which has been experimentally validated using double vacuum glazing
66 (DVG) samples [19, 20] a three-dimensional finite volume model to simulate the thermal performance of the entire
67 TVG was developed. In this model, the support pillar arrays within the two vacuum gaps were incorporated and
68 modelled directly. The circular cross section of the pillar in a fabricated system was modelled as a square cross
69 section pillar of equal area in the model. It has been proven that the heat flow through the square and circular
70 support pillars with the same cross sectional areas is the same [18]. An optimized mesh is generated with a high
71 density of nodes in and around the pillar to provide high accuracy for the heat transfer calculation. Using this finite
72 volume model, Fang et al. [20] investigated the effect of vacuum gap edge seal material and width, frame rebate

depth and glazing size on the thermal performance of the TVG. In previous research on DVG, this finite volume model has been employed to investigate the effect of hard and soft low-e coatings on the thermal performance of DVG and has been experimentally validated [21].

The objective of this paper is to theoretically and experimentally investigate the effects of the emittance value and the number and location of the low-e coated surfaces within the vacuum gaps on the thermal performance of the TVG. Based on the investigation results, optimisation for the low-e coating position on glass surfaces 2-5 (Fig. 1) within two vacuum gaps is then achieved when using one to three low-e coatings in the TVG.

NOMENCLATURE

a	Radius of support pillar (m)
h	Surface heat transfer coefficient ($\text{W.m}^{-2}.\text{K}^{-1}$)
k	Thermal conductivity ($\text{W.m}^{-1}.\text{K}^{-1}$)
p	Pillar separation (m)
R	Thermal resistance ($\text{m}^2.\text{K}.\text{W}^{-1}$)
t	Thickness of glass pane (m)
T	Temperature ($^{\circ}\text{C}$)
U	Thermal transmission ($\text{W.m}^{-2}.\text{K}^{-1}$)
Greek letters	
ε	Hemispheric emittance of a surface
σ	Stefan-Boltzmann constant ($5.67 \times 10^{-8} \text{W.m}^{-2}.\text{K}^{-4}$)
Δ	Mean surface temperature difference between glass panes I, II, III.
Subscripts	
$1 \text{ to } 6$	Refer to surfaces of glass panes shown in Fig. 1
I, II, III	Refer to the first, second and third glass panes
i, o	Refer to warm and cold ambient temperatures
g	Glass
m	Glass pane number of the TVG
n	Vacuum gap number
p	Pillar
r	Radiation
tot	Total resistance of triple vacuum glazing

2. RESEARCH METHODOLOGY

The methodology adopted in this research was to use analytic and finite element models to investigate the thermal performance of TVG with a range of low-e coatings. A number of TVGs with various coating setting methods were fabricated and their U-values experimentally determined by using a guarded hot box calorimeter developed at Ulster University. The experimentally determined U-values are compared with the simulation results.

2.1 HEAT TRANSFER THROUGH TVG

The schematic diagram of a TVG cross section showing heat transfer mechanisms through the glazing components is shown in Fig. 1, which is not to scale. The support pillars and vacuum gap widths are significantly exaggerated.

(Fig. 1)

Fig. 1 shows the heat transfer across the TVG by: 1) conduction and radiation from the indoor ambient to the glass pane surface 6, 2) conduction across the indoor side glass pane to surface 5; 3) radiation between surfaces 5 and 4, conduction through the pillar array within vacuum gap 2 and heat conduction through the edge seal of vacuum gap 2; 4) conduction across the middle glass pane from surface 4 to surface 3; 5) radiation between surfaces 3 and 2, conduction through the pillar array within vacuum gap 1 and conduction through the edge seal of vacuum gap 1; 6) conduction across the outdoor glass pane from surface 2 to surface 1; 7) convection and radiation from the cold side surface 1 to the cold ambient. The analytic and finite element models for analysing the heat flow through the centre-of-glazing were established by Manz et al. [18]. The heat transmissions calculated by both models were in very good agreement.

2.2 ANALYTIC MODEL APPROACH

Due to symmetry, the analysis of the unit cell allowed for a reduction in the computer simulation time for the overall glazing. The influence of low-e coating on TVG thermal performance was analysed using the thermal network [18, 20] of a 25 mm by 25 mm unit cell with a pillar in the centre at the centre-of-glazing area and is presented in Fig. 2 (a) and (b).

(Fig. 2)

The thermal resistance associated with the heat flow per m^2 due to heat conduction of each glass pane is given by:

$$R_{g,m} = \frac{t_m}{k_g} \quad (1)$$

where t_m is the thickness of glass pane m , where $m \in (I, II, III)$, k_g is the thermal conductivity of glass.

The thermal resistance associated with radiative heat flow between the glass surfaces within each of the vacuum gaps is:

$$R_{r,1} = \left(\frac{1}{\varepsilon_2} + \frac{1}{\varepsilon_3} - 1 \right) (4\sigma T_{2,3}^3)^{-1} = (4\varepsilon_{2,3}\sigma T_{2,3}^3)^{-1} \quad (2)$$

$$R_{r,2} = \left(\frac{1}{\varepsilon_4} + \frac{1}{\varepsilon_5} - 1 \right) (4\sigma T_{4,5}^3)^{-1} = (4\varepsilon_{4,5}\sigma T_{4,5}^3)^{-1} \quad (3)$$

where $\varepsilon_2, \varepsilon_3, \varepsilon_4$ and ε_5 are the hemispheric emittance of glass surfaces 2, 3, 4, and 5 within vacuum gaps 1 and 2 as shown in Figs. 1 and 2; the $\varepsilon_{2,3}$ and $\varepsilon_{4,5}$ are combined effective emittances of surfaces in vacuum gaps 2 and 1; σ is the Stefan-Boltzmann constant; $T_{2,3}$ and $T_{4,5}$ are the mean temperatures in Kelvin of glass surfaces 2, 3 and 4, 5 respectively in vacuum gaps 1 and 2. The thermal resistance associated with the heat conduction through the support pillars in vacuum gap n (1 or 2) is determined by equation 4 [13]:

$$R_{p,n} = \frac{p^2}{2k_g a} \quad (4)$$

where a is the radius of the cylindrical pillar. The thermal resistance of the middle glass pane is divided into two equal thermal resistances, therefore the total thermal resistance associated with the heat flow between surfaces 1 and 6 is determined by equation 5:

$$R_{tot} = \frac{R_{p,1}(R_{g,1} + R_{r,1} + \frac{1}{2}R_{g,II})}{R_{p,1} + R_{g,1} + R_{r,1} + \frac{1}{2}R_{g,II}} + \frac{R_{p,2}(R_{g,III} + R_{r,2} + \frac{1}{2}R_{g,II})}{R_{p,2} + R_{g,III} + R_{r,2} + \frac{1}{2}R_{g,II}} \quad (5)$$

The thermal resistances associated with the heat flows R_i and R_o at the glazing surfaces 6 and 1 are the inverse of the surface heat transfer coefficients, i.e. $R_i = 1/h_i$ and $R_o = 1/h_o$. The total heat transmission [18] of the unit cell at the centre-of-glazing area is then given by:

$$U_{tot} = \frac{1}{R_i + R_{tot} + R_o} \quad (6)$$

The heat flow through the entire TVG is the sum of heat flow across the centre-of-glazing area where the combined effective emittances of surfaces in gaps 1 and 2 play the significant role as shown by equations 2 and 3

and the heat flow through the edge area including the heat conduction through the edge seal, whose analytic model is presented in the literature [13].

2.3 FINITE VOLUME APPROACH

The finite volume model of Fang et al., [19] for DVG was adapted to suit the structure of TVG. The heat transmission calculated for TVG using this finite volume model was in very good agreement with that of Manz et al [18] and Fang et al. [20]. The detailed description for the finite volume model is presented in Fang et al., [21]. The simulated thermal transmission of a standard unit containing a pillar in the centre of a 25 mm by 25 mm centre-of-glazing area was in good agreement with the result calculated using the analytical model with a 1.8% variation [20] which is comparable with the variation (2%) of Manz et al. [18]. With the 85×85 nodes distributed on the y and z directions on the glazing surface and with 20 nodes on the x direction, the U-value at the centre-of-glazing for DVG with emittance of 0.02 was determined to be $0.36 \text{ W.m}^{-2}.\text{K}^{-1}$ with two low-e coated 6 mm thick glass panes. This is comparable to the findings of Griffiths et al. [15], Fang et al. [20] and Manz et al. [18]. This level of agreement is satisfactory to simulate a practical heat flow with high accuracy.

3. INFLUENCE OF LOW-E COATINGS ON THE THERMAL PERFORMANCE OF TVG

The simulated TVGs consisted of three 4 mm thick glass panes, sealed by two indium alloy based edge seals 6 mm wide and rebated into a solid wood frame with a rebate depth of 10 mm as shown in Fig. 1. The two 0.12 mm wide vacuum gaps were maintained by two pillar arrays with a pillar diameter of 0.3 mm and spaced at 25 mm. The thermal conductivity of indium alloy, glass, pillar and wood frame were $83.7 \text{ W.m}^{-1}.\text{K}^{-1}$, $1 \text{ W.m}^{-1}.\text{K}^{-1}$, $20 \text{ W.m}^{-1}.\text{K}^{-1}$ and $0.17 \text{ W.m}^{-1}.\text{K}^{-1}$ respectively. In the simulation the air temperatures in the hot and cold sides were 20 °C and 0 °C; the glazing surface heat transfer coefficients at the hot and cold sides were $7.7 \text{ W.m}^{-2}.\text{K}^{-1}$ and $25 \text{ W.m}^{-2}.\text{K}^{-1}$ respectively in accordance with the requirement of ISO standard 10077-1[22].

3.1 SIMULATED TVG THERMAL PERFORMANCE WITH FOUR LOW-E COATINGS

With these boundary conditions and configuration parameters the thermal performance of TVG with four low-e coatings of 0.03 and 0.18 emittance were calculated. The use of four coatings within the TVG is the best case scenario. With the boundary conditions above and configuration parameters, the 3-D isotherms of the 0.4 m by 0.4 m TVG with four 0.03 emittance coatings were calculated and are illustrated in Fig. 3, which show the temperature gradient across the three glass panes due to the high thermal resistance of the two vacuum gaps.

(Fig. 3)

For a TVG with four low-e coatings of 0.03 emittance, the U-values of the centre-of-glazing and total glazing areas are $0.22 \text{ W.m}^{-2}.\text{K}^{-1}$ and $0.64 \text{ W.m}^{-2}.\text{K}^{-1}$, which are comparable to the result of Manz et al. [18]. For a TVG with four low-e coatings with emittance of 0.18 emittance, the U-values of the centre-of-glazing and total glazing areas are $0.41 \text{ W.m}^{-2}.\text{K}^{-1}$ and $0.80 \text{ W.m}^{-2}.\text{K}^{-1}$. The mean surface temperature difference between the indoor and outdoor glass panes, that between the indoor and middle glass panes; that between the outdoor and middle glass panes for the TVG with emittance of 0.03 and 0.18 are listed in Table 1.

(Table 1)

The temperature difference between the indoor and outdoor glass panes with an emittance of 0.03 is $1.4 \text{ }^{\circ}\text{C}$ higher than that with an emittance of 0.18. Equations 2 and 3 show that although the effective emittances $\varepsilon_{2,3}$ and $\varepsilon_{4,5}$ of the two opposite surfaces within vacuum gaps 1 and 2 are equal, a difference in the mean temperatures $T_{2,3}$, and $T_{4,5}$ of glass surfaces 2, 3 and 4, 5 in vacuum gaps 1 and 2 results in a difference in the thermal resistances $R_{l,r}$, and $R_{2,r}$ of vacuum gaps 1 and 2.

The U-values at the centre-of-glazing and total glazing areas of 0.4 m by 0.4 m and 1 m by 1 m TVGs with four low-e coatings with emittance between 0.03 and 0.18 rebated within a solid wooden frame with a 10 mm rebate depth are shown in Fig. 4. For comparison, the U-values of 0.4 m by 0.4 m and 1 m by 1 m DVG with two low-e coatings with emittances between 0.03 and rebated within a solid wood frame with a 10 mm rebate depth are also included in Fig. 4.

(Fig. 4)

Fig. 4 shows that if using 0.18 emittance low-e coatings, the difference in U-value between the DVG and TVG with dimensions of 0.4 m by 0.4 m or 1 m by 1 m is larger than that if using 0.03 emittance low-e coatings. The difference in U-value at the total glazing area between the 1 m by 1 m TVG and DVG is larger than that between the 0.4 m by 0.4 m TVG and DVG. Fig. 4 also shows that the difference in U-value of the total glazing area between the 0.4 m by 0.4 m and 1 m by 1 m TVGs is much larger than that between the 0.4 m by 0.4 m and 1 m by 1 m DVG, since lateral heat conduction through the edge area of the TVG is larger than that of the DVG. This indicates that larger size TVGs have a greater advantage over smaller size TVGs in comparison to the DVG. Fig. 4 also shows that the U-values at the centre-of-glazing area for 0.4 m by 0.4 m and 1 m by 1 m TVG are the same; while the U-values at the centre-of-glazing area for 0.4 m by 0.4 m and 1 m by 1 m TVG are very close with a difference of less than $0.03 \text{ W.m}^{-2}.\text{K}^{-1}$. For the TVG, the influence of the lateral heat conduction through the edge seal on the U-value at the centre-of-glazing area is larger than that in the DVG. The influence of lateral heat conduction on the U-value at the centre-of-glazing area of the 0.4 m by 0.4 m TVG is larger than that of the 1 m by 1 m TVG, leading to an increase in the U-value at the centre-of-glazing area of the 0.4 m by 0.4 m TVG compared to the 1 m by 1 m TVG, nevertheless this difference is very small.

3.2 SIMULATED TVG THERMAL PERFORMANCE WITH THREE LOW-E COATINGS

In the first stage of TVG fabrication, a low-e coated glass is used with one coating in one vacuum gap and with two coatings in the second vacuum gap with a 10 mm frame rebate depth within a solid wood frame. In the simulation, two scenarios were considered for the orientation of the low-e coatings. In method 1, surfaces 2 and 3 in the cold side vacuum gap and surface 5 in the warm side vacuum gap were low-e coated as shown in Fig. 1. In method 2, surface 2 in the cold side vacuum gap and surfaces 4 and 5 in the warm side vacuum gap were low-e coated. The U-values at the centre-of-glazing and total glazing areas of the TVGs with 0.4 m by 0.4 m and 1 m by 1 m dimensions and three low-e coatings with emittance between 0.03 and 0.18 with setting methods 1 and 2 were calculated and are presented Fig. 5.

(Fig. 5)

Fig. 5 shows that for the TVG with three low-e coatings, the difference in U-values at the centre-of-glazing area between 0.4 m by 0.4 m and 1 m by 1 m TVG with setting methods 1 and 2 is negligible. The difference in U-values of the total glazing areas of the 0.4 m by 0.4 m and 1 m by 1 m TVGs with 0.18 emittance coatings is larger than that with 0.03 emittance coatings, although this difference is very small. These results indicate that when using three 0.18 emittance coatings in a TVG, setting method 2 provides a lower U-value than setting method 1; when using three 0.03 emittance coatings, the setting method is less important compared to using 0.18 emittance coatings. For 0.4 m by 0.4 m TVG with three 0.03 emittance coatings, the difference in U-value of the total glazing area between the setting method 1 and 2 is negligible.

3.3 SIMULATED THERMAL PERFORMANCE OF TVG WITH TWO LOW-E COATINGS

The U-values of 0.4 m by 0.4 m and 1 m by 1 m TVGs with two low-e coatings with emittances between 0.03 and 0.18 were simulated and are presented in Figs. 6 and 7. Three setting methods of the two low-e coatings were considered. Setting method 3: surfaces 5 in the warm side and 2 in the cold side vacuum gaps were low-e coated; Setting method 4: surfaces 3 and 2 in the cold side vacuum gap were low-e coated; Setting method 5: surfaces 4 and 5 in the warm side vacuum gap were low-e coated. The U-value of 0.4 m by 0.4 m and 1 m by 1 m TVGs with 0.03 emittance coatings using the three setting methods are compared in Fig. 8.

(Fig. 6)

Fig. 6 shows that for 0.4 m by 0.4 m TVG with two coatings, setting one coating in both of the vacuum gaps (setting method 3) gives the lowest U-value, while setting two coatings in the cold side vacuum gap (setting method 4) gives the highest U-value; the U-value of the TVG with two coatings in the warm side vacuum gap (setting

method 5) is in between. These are reflected by the temperature differences between the warm side and cold side glass panes in setting methods 3, 4, 5, which are 10.5 °C, 8.6 °C and 9.3 °C respectively. These results are in good agreement with those calculated using equations 1 to 6 of the analytic model explained in section 2.1.

(Fig. 7)

Fig. 7 shows that when using two coatings in TVG, setting one coating in each vacuum gap at surfaces 5 and 2 will give lowest U-value. Comparing Figs. 6 and 7, it can be seen that the difference in U-values for setting methods 3, 4 and 5 for the 0.4 m by 0.4 m TVG is larger than that for the 1 m by 1 m TVG. This means that for 0.4 m by 0.4 m TVG with two low-e coatings, the influence of setting method is more significant compared to the 1 m by 1 m TVG. This is due to increased lateral heat transfer through the edge area of the 0.4 m by 0.4 m TVG compared to that of the 1 m by 1 m TVG.

(Fig. 8)

Fig. 8 shows that with setting methods 3 and 5, the U-values at the centre-of-glazing of 0.4 m by 0.4 m and 1 m by 1 m TVGs with two 0.03 emittance coatings are approximately the same; while with setting method 4, the U-value at the centre-of-glazing of 0.4 m by 0.4 m TVG is larger than that of the 1 m by 1 m TVG. This is because in method 4, there is increased lateral heat conduction from the warm side glass pane to the middle and cold side glass panes compared to that in methods 3 and 5, and therefore the U-value at the centre-of-glazing area of 0.4 m by 0.4 m TVG is larger than that of 1 m by 1 m TVG.

3.4 SIMULATED THERMAL PERFORMAMNCE OF TVG WITH ONE LOW-E COATING

When using only one coating with an emittance of 0.03 in the 0.4 m by 0.4 m TVG, the U-values at the centre-of-glazing and total glazing areas were calculated and are illustrated in Fig. 9. Two setting methods were considered: method 6, one low-e coating in the cold side vacuum gap on surface 2; method 7, one low-e coating in the warm side vacuum gap on surface 5. The U-values of 0.4 m by 0.4 m and 1 m by 1 m TVGs with both setting methods are compared in Fig. 10.

(Fig. 9) (Fig. 10)

Figure 9 shows that the U-value of the 0.4 m by 0.4 m TVG with setting method 7 is lower than that with setting method 6, since the low-e coating at the warm side glass pane surface can more efficiently reduce the radiative heat transfer across the TVG than that with the coating at the cold side glass pane. Fig. 10 shows that the U-values at both the centre-of-glazing and total glazing area of the 1m by 1 m TVG with one coating in the cold side vacuum gap are higher those with one coating in the warm side vacuum gap. The difference in U-value of the total glazing

area from using the two setting methods is larger for the 0.4 m by 0.4 m TVG compared to the 1 m by 1 m TVG. Fig. 10 also shows that with one coating in the warm side vacuum gap, the U-value at the centre-of-glazing area of the 0.4 m by 0.4 m and 1 m by 1 m TVG are approximately same, but with one coating in the cold side vacuum gap, the U-value at the centre-of-glazing area of the 0.4 m by 0.4 m TVG is larger than that of the 1 m by 1 m TVG. This is because: firstly, with no coating in the warm side vacuum gap, radiative heat transfer across the warm side vacuum gap is significant; Secondly, increased radiative heat transfer from the warm side glass pane to the middle glass pane is then conducted through the edge seal to the cold side glass panes by lateral heat transfer, leading to an increased U-value at the centre-of-glazing for the 0.4 m by 0.4 m TVG compared to the 1 m by 1 m TVG. When the single coating is set in the warm side vacuum gap in both 0.4 m by 0.4 m and 1 m by 1 m TVGs, the lateral heat transfer through the edge seal is much smaller than that when the single coating is set in the cold side vacuum gap. This indicates that setting the low-e coating at the warm side glass pane is very important for reducing the overall heat transfer through the glazing.

3.5 SIMULATED THERMAL PERFORMANCE OF TVG WITH ONE, TWO, THREE AND FOUR LOW-E COATINGS

The U-values of the 0.4 m by 0.4 m and 1 m by 1 m TVGs with one coating at surface 5, two at surfaces 2 and 5, three at surfaces 3, 4, and 5 and four at surfaces 2, 3, 4 and 5 with emittance of 0.03 and 0.18 are compared in Figs. 11 and 12. Based on the number of coatings within the TVG the setting methods giving a lowest thermal transmittance are selected.

(Fig. 11) (Fig. 12)

Figures 11 and 12 show that the U-value decreases with increasing the number of low-e coatings. The difference in U-value between TVGs with one and two coatings is much larger than that of the TVGs with two and three coatings. The difference in U-value at both the centre-of-glazing and total glazing areas of TVGs with two and three low-e coatings is larger than that of TVGs with three and four low-e coatings. This indicates that the impact of the number of low-e coatings has on the thermal performance of TVG decreases with an increasing number of coatings. In Fig. 11, the difference in U-value at centre-of-glazing and total glazing areas of TVGs with three and four 0.03 emittance coatings is small. Therefore when applying 0.03 emittance coatings, using two coatings (one in both vacuum gaps) is more practical than using three low-e coatings in the TVG due to increased solar heat gain and visible light transmission. Comparing Fig. 11 and Fig. 12 it can be seen that the difference in U-value of TVG as a result of increasing the number of 0.18 emittance coatings is larger than that as a result of increasing the number of 0.03 emittance coatings. This is because the U-value of the TVG with 0.03 emittance coatings is much lower than that with 0.18 emittance coatings. When using 0.18 emittance coatings in a TVG, applying three coatings is practical in terms of thermal performance improvement when using the best coating setting method.

4. EXPERIMENTAL VALIDATION OF THE THERMAL PERFORMANCE OF TVG WITH TWO AND THREE LOW-E COATINGS

Fabricating TVG requires the formation of a leak-free seal around its perimeter; this is accomplished by bonding the three glass sheets together with indium using an ultrasonic soldering process and the application of a secondary seal to prevent moisture ingress from occurring. This technique, developed at the Ulster University [15, 16, 14], enables TVG to be produced at a temperature of less than 160°C.

The sealing of the glass panes is carried out in a vacuum oven in which the glazing is heated up to 160°C. Prior to fabrication, a hole is drilled in two of the glass panes; one hole in the upper glass pane for evacuation purpose and another hole in the middle pane which separates the two vacuum spaces. After the edge seal formation and subsequent cool down of the glazing assembly, a turbo molecular vacuum pump is connected to the glazing via a pump-out cup which uses an O-ring seal on the upper glass sheet around the pump out hole. During evacuation the glazing assembly is re-heated to 150°C in a bake-out oven to outgas the internal glazing surfaces. After evacuation is completed the pump-out hole is sealed using a glass cover disc pre-coated in indium which has been described in detail elsewhere [16]. Fig. 13 shows a schematic diagram of a TVG. The fabricated glazing comprises three 4 mm thick glass panes, 0.4 m by 0.4 m, with low-e coatings with emittance of 0.18 on one or more of the internal glass surfaces. The glass sheets, separated by arrays of tiny support pillars on a regular square grid, are sealed together around the edges to form narrow evacuated spaces. The support pillars, made of stainless steel have a diameter of 0.4mm and a height of 0.15 mm.

(Fig. 13)

Two 0.4 m by 0.4 m TVGs with three, 4 mm thick glass panes were fabricated using the method detailed by Arya et al. [17]. Three low-e coated glass panes with emittance of 0.18 were used within the first TVG and two low-e coated glass panes with emittance of 0.18 in the second TVG. The U-values of the TVG were experimentally determined using a guarded hot box calorimeter [19] as shown in Fig. 14. The hot box calorimeter was designed in accordance with the British Standard methods for determining the thermal insulating properties [24] and the international standard [25]. The calorimeter comprises a hot and cold chamber separated by a mask wall. An opening is provided in the centre of the mask wall where a frame is installed which can accommodate a TVG of 0.4 m by 0.4 m. Electrical heaters and fans are used to create a uniform temperature in the chambers. A metering box is located inside the hot chamber in which the air temperature is accurately controlled and a steady state condition ($\pm 0.1^\circ\text{C}$) is created. The air temperature in the hot chamber is the same as that in the metering box to minimise heat exchange between the chambers. A chiller and fans have been installed inside the cold chamber which provides a uniform low temperature environment. For given air temperatures within the cold and hot chambers the hot box calorimeter allows an accurate measurement of the heat flow through the panel. The calculation method for the U-value of the test sample is reported elsewhere [19]. The system error of the guarded hot box calorimeter is $\pm 5\%$ [19].

(Fig. 14) (Fig. 15)

Two tests were undertaken for the first TVG, i) the three coatings were set at surfaces 2, 3 and 5, which is referred to as TVG1; ii) the three coatings were set at surfaces 2, 4, and 5, which is referred to as TVG2. As an example, the isotherms of the TVG2 installed within the guarded hot box calorimeter were measured using an infrared camera and are presented in Fig. 15, in which the heat conduction through the support pillars indicates the high vacuum has been achieved.

Two tests were undertaken for the second TVG: iii) two coatings were set at surfaces 2 and 3, which is referred to as TVG3; iv) two coatings were set at surfaces 4 and 5, which is referred to as TVG4. The experimentally determined U-values are presented in Table 4. The ambient conditions are listed in Table 3. A double vacuum glazing was fabricated using the pump out method [16] and characterised using the guarded hot box and presented in Table 2 as a comparison.

(Table 2) (Table 3)

Table 2 shows that the experimentally determined and predicted U-values are in very good agreement. Although the U-values at the centre-of-glazing area of the 0.4 m by 0.4 m TVG are much lower than that of the DVG, the difference in U-value of the total glazing areas between the DVG and TVG is less than that at the centre-of-glazing area. This is because the lateral heat conduction through the edge of TVG is larger than that of DVG, which compromises the U-value of the total glazing area of the TVG. As there is no low-e coating in the warm side vacuum gap for TVG3, the edge effect is larger than that for TVG4 which has two low-e coatings in the warm side vacuum gap.

5. RESULTS AND DISCUSSIONS

The simulated U-values of the 0.4 m by 0.4 m and 1 m by 1 m TVGs with three low-e coatings with emittance of 0.03 and 0.18 are listed in Table 4. Method 1 refers to coatings at surfaces 2, 3 and 5; Method 2 refers to coatings at surfaces 2, 4 and 5.

(Table 4)

The simulation results show that for both sizes of TVG with three low-e coatings, the TVG with setting method 2 achieved a lower U-value than method 1, i.e. two low-e coatings should be set in the warm side vacuum gap, while one coating set in the cold side vacuum gap. This is due to the greater thermal resistance of the vacuum gap with two low-e coatings at the warm indoor environment. With two low-e coatings within a TVG, the U-values at the centre-

of-glazing and total glazing areas of the 0.4 m by 0.4 m and 1 m by 1 m TVG with an emittance of 0.03 and 0.18 when using setting methods 3, 4, and 5 are listed in Tables 5 and 6.

(Table 5) (Table 6)

Tables 5 and 6 show that for both 0.4 m by 0.4 m and 1 m by 1 m TVGs, setting one low-e coating in each of the vacuum gaps, method 3 gives significantly lower U-value compared to setting both coatings in the same vacuum gap. The U-values of 0.4 m by 0.4 m TVG with a single coating with emittance of 0.03 and 0.18 at surface 2 or at surface 5 are listed Table 7.

(Table 7)

Table 7 shows that a single low-e coating at surface 5 gives a lower U-value than when positioned at surface 2, hence the single coating should be set in the warm side vacuum gap. The location of low-e coatings within the TVG is significant for achieving a low U-value. The U-value at the centre-of glazing and total glazing areas of 0.4 m by 0.4 m TVG with no low-e coatings are $1.46 \text{ W.m}^{-2}.\text{K}^{-1}$ and $1.70 \text{ W.m}^{-2}.\text{K}^{-1}$ respectively, which are significantly larger than those of the U-values of the TVG with a single coating at surface 2 or 5. Comparing these U-values to the U-values in table 4, 5, 6 and 7, it can be seen that the reduction in U-value due to the inclusion of the first coating is the largest, which decreases accordingly with the inclusion of the second, third and fourth coatings.

The experimentally determined U-values of 0.4 m by 0.4 m TVG with setting methods 1, 2, 4 and 5 are in very good agreement with the simulation results. The experimental validation for a large sample with dimensions of 1 m by 1 m will be undertaken in the next stage of the work.

6. CONCLUSION

The influence of emittance and location of low-e coatings on the thermal performance of 0.4 m by 0.4 m and 1 m by 1 m TVGs with a 10 mm frame rebate were simulated using a finite volume model. The TVG comprised three 4 mm thick glass panes with two vacuum gaps and a 6 mm wide indium alloy edge seal. In the simulation, the two vacuum gaps were separated by support pillars with a diameter of 0.3 mm, height of 0.2 mm and spaced at 25 mm.

The simulations and experimental validation have shown that in a heating dominated climate, when using three low-e coatings in the TVG, the vacuum gap with two low-e coatings should be set facing the warm side (indoor) environment; while the vacuum gap with one low-e coating should face the cold side (outdoor) environment. This is because the vacuum gap with two low-e coatings at the warm side can exhibit higher thermal resistance compared to the vacuum gap with two low-e coatings at the cold side environment. In a cooling dominated climate, the vacuum gap with two low-e coatings should be set facing the outdoor (hot) environment, while the vacuum gap with one low-e coating should face the indoor (cool side) environment.

When using just two low-e coatings in a TVG, setting one coating in both vacuum gaps gives a significantly lower U-value compared to setting both coatings in the same vacuum gap. This result is valid for both heating and

cooling dominated climates. Setting two coatings in the warm side vacuum gap gives a lower U-value than setting two coatings in the cold side vacuum gap. Using one low-e coating in the TVG compromises the advantage of the two vacuum gaps, thus it is not practical for a TVG application.

The location of low-e coatings within the TVG is significant for achieving a low U-value. The first coating in the vacuum gap at the warm side glass pane is most efficient at reducing radiative heat transfer across the TVG. The relative impact of the second, third and fourth low-e coatings on reducing the U-value of the TVG decreases accordingly. This conclusion can be practically applied in the fabrication of TVG. Without incurring extra cost, the correct setting of low-e coating secures better thermal performance of the TVG.

ACKNOWLEDGEMENT

The authors acknowledge the support from the Charles Parson Energy Research Awards through the National Development 2007-2014 of the Department of Communications, Marine and Natural Resources, Dublin, Ireland. The support from EC POREEN project: FP7-MC-IRSES (grant agreement No. 318908) is appreciated.

REFERENCE

- [1] Zoller A., Hohle Glasscheibe. German Patent Application No. 387655, 1913.
- [2] Benson D.K., Tracy C.E., Laser sealed vacuum insulation window. U.S. Patent Number 4,683,154. 28 June 1987.
- [3] Kreisman W.S., Method of fabricating a thermal pane window and product. U.S. Patent No. 4,393,105. 12 Jul 1983.
- [4] Robinson S. J. and Collins R.E., Evacuated windows-theory and practice, *ISES Solar World Congress, International Solar Energy Society*, 1989, Kobe, Japan.
- [5] Parker K. R., Insulating glazing unit. Canadian Patent Number 1,290,624. 1991.
- [6] Demars Y., Gobain S., Process for producing a vacuum in an insulating glazing. U.S. Patent No. 5,855,638. 5 Jan 1999.
- [7] Landa K., Landa L., Aggas S., Wang Y., Vacuum IG unit with alkali silicate edge seal and / or spacers. U.S. Patent Number 6,541,083. 1 Apr 2003.
- [8] Sager-Hintermann K., Baechli E., Method and equipment for making heat-insulating construction and/or lighting element. European Patent No. 1221526, 2002.

- [9] Wittwer V., Private communicate, 2005, Fraunhofer Institute for Solar Energy Systems, Freiburg, Germany.
- [10] Stark D., Insulated glazing units. U.S. Patent No. 7,832,177. 16 Nov. 2010.
- [11] Francis, IV., Freebury G.E., Beidleman N.J., Hulse M. Method and apparatus for an insulating glazing unit and compliant seal for an insulating glazing unit. U.S. Patent No. 0279,170. 8 Nov 2012.
- [12] Friedl W., ProVIG production technologies for vacuum insulated glass, Glasstec Symposium, September 2010, Dusseldorf, Germany
- [13] Collins R.E., and Simko T.M. Current Status of the Science and Technology of VG. Solar Energy, 62, 189-213, 1998.
- [14] Griffiths P. W., Di M. Leo Di M., Cartwright P., Eames P. C., Yianoulis P., Leftheriotis G., Norton B. Fabrication of evacuated glazing at low temperature. Solar Energy 63, 243-249, 1998.
- [15] Hyde T.J., Griffiths P.W., Eames P.C., Norton B. Development of a novel low temperature edge seal for evacuated glazing. In Proc. World Renewable Energy Congress VI, U.K. pp. 271-274, 2000.
- [16] Zhao J. F, Eames P.C., Hyde T.J., Fang Y., Wang J., A modified pump-out technique used for fabrication of low temperature metal sealed vacuum glazing. Solar Energy 81, 1072-1077, 2007.
- [17] Eames P.C., Vacuum glazing: Current performance and future prospects. Vacuum, 82(7), 717-722, 2008.
- [18] Manz H., Brunner S., Wulschlegler L., Triple vacuum glazing and basic mechanical design constraints. Solar Energy 80 1632-1642, 2006.
- [19] Fang Y., Eames P.C., Norton B., Hyde T.J., Experimental validation of a numerical model for heat transfer in evacuated glazing. Solar Energy 80, 564-577, 2006.
- [20] Fang Y., Hyde T.J., Hewitt N., Predicted thermal performance of triple vacuum glazing. Solar Energy 84, 2132-2139, 2010.
- [21] Fang Y., Eames P.C., Norton B., Hyde T.J., Zhao J., Wang J. Huang Y., Low emittance coatings and the thermal performance of vacuum glazing. Solar Energy 81, 8-12, 2007.

[22] EN ISO 10077-1, Thermal performance of windows, doors and shutters - Calculation of thermal transmittance - Part 1: Simplified method. European Committee for Standardization CEN, Brussels, 2006.

[23] Arya F., Fang Y., Hyde T.J., Fabrication and characterization of triple vacuum glazing at low temperature using an indium-based seal. Proceeding of “The Energy & Materials Research Conference (EMR2012)” Malaga Spain 20-22 June 2012. (available in CD)

[24] British Standards Institution, Determining Thermal Insulating Properties, Part 3. Test for Thermal Transmittance and Conductance, Section 3.1 Guarded Hot-box Method. British Standards Institution, Chiswick, London, UK. 1987.

[25] International Standard Organization, BS EN ISO 8990, Thermal insulation- Determination of steady-state thermal transmission properties - Calibrated and guarded hot box. 1996.

Fig. 1 Schematic diagram of a TVG cross section and heat flow mechanism across the TVG.

Fig. 2 Schematics of a quarter of a unit cell (a) and its thermal network at the central glazing area (b).

Fig. 3 Isotherms of TVG with four 0.03 emittance low-e coatings.

Fig. 4 U-value of the TVGs with four low-e coatings of various emittances.

Fig. 5 U-value at centre-of-glazing and total glazing areas of TVGs with three low-e coatings.

Fig. 6 U-values at the centre-of-glazing and the total glazing areas of the 0.4 m by 0.4 m TVGs with two low-e coatings.

Fig. 7 U-values at the centre-of-glazing and the total glazing areas of the 1 m by 1 m TVGs with two low-e coatings in setting methods 3, 4, 5.

Fig. 8 Comparison of U-value of TVGs with two 0.03 emittance coatings using different setting methods.

Fig. 9 U-values of 0.4 m by 0.4 m TVGs with one low-e coating in the warm and cold side vacuum gaps.

Fig. 10 U-values of TVGs with one 0.03 emittance low-e coating.

Fig. 11 Comparison of U-values of TVG with one, two, three and four 0.03 emittance coatings.

Fig. 12 Comparison of U-values of TVG with one, two, three and four 0.18 emittance coatings.

Fig. 13 Schematic diagram of TVG fabricated based using an indium edge seal and pump-out technique.

Fig. 14 Guarded hot box calorimeter available at Ulster University.

Fig. 15 Isotherms of TVG2 installed within the guarded hot box calorimeter measured using an infrared camera.

Table 1. Simulated thermal performance of TVGs with four low-e coatings.

Glazings with four low-e coatings	TVG1	TVG2
Emittance	0.03	0.18
Centre of glazing U-value ($\text{W.m}^{-2}.\text{K}^{-1}$)	0.22	0.41
Total glazing U-value ($\text{W.m}^{-2}.\text{K}^{-1}$)	0.64	0.80
$\Delta T_{\text{I,III}}$ (°C)	10.8	9.4
$\Delta T_{\text{II,III}}$ (°C)	7.5	5.8
$\Delta T_{\text{I,II}}$ (°C)	3.3	3.6

Table 2 Comparison of the predicted and experimentally measured U-values of the TVG with two and three 0.18 emittance low-e coatings.

Number of coatings	DVG & TVG	Predicted U-value (W.m ⁻² .K ⁻¹)		Measured U-value (W.m ⁻² .K ⁻¹)	
		Central glazing	Total glazing	Central glazing	Total glazing
2	DVG	0.85	1.12	0.88	1.16
3	TVG1 (method 1)	0.50	0.88	0.53	0.91
	TVG2 (method 2)	0.46	0.85	0.48	0.88
2	TVG3 (method 4)	0.72	1.10	0.77	1.14
	TVG4 (method 5)	0.59	0.97	0.60	0.98

Table 3 Ambient conditions in the guarded hot box calorimeter.

Sample type	Air temperature (°C)		Surface heat transfer coefficient (W.m ⁻² .K ⁻¹)	
	Hot box	Cold box	Hot box	Cold box
DVG	19.0	-0.3	5.79	17.91
TVG1	18.2	-0.3	6.59	14.94
TVG2	18.2	-0.3	6.59	15.13
TVG3	17.5	-0.3	9.41	19.41
TVG4	17.6	-0.3	8.62	17.12

Table 4 U-values of 0.4 m by 0.4 m and 1 m by 1 m TVGs with three low-e coatings in setting methods 1 and 2.

Low-e coating setting method	0.4 m by 0.4 m TVG U-value (W.m ⁻² .K ⁻¹)			
	Emittance: 0.03		Emittance: 0.18	
	Central glazing	Total glazing	Central glazing	Total glazing
Method 1	0.25	0.66	0.50	0.88
Method 2	0.23	0.65	0.46	0.85
	1 m by 1 m TVG U-value (W.m ⁻² .K ⁻¹)			
	Central glazing	Total glazing	Central glazing	Total glazing
Method 1	0.24	0.50	0.48	0.72
Method 2	0.22	0.48	0.45	0.69

Table 5 U-values of the 0.4 m by 0.4 m TVG with emittance of 0.03 and 0.18 in setting methods 3, 4 and 5.

Low-e coating setting method	U-value ($\text{Wm}^{-2}\text{K}^{-1}$)			
	Emittance: 0.03		Emittance: 0.18	
	Central glazing	Total glazing	Central glazing	Total glazing
Method 3	0.25	0.67	0.57	0.94
Method 4	0.50	0.93	0.72	1.10
Method 5	0.33	0.76	0.59	0.97

Table 6 U-values of the 1 m by 1 m TVG with emittance of 0.03 and 0.18 in setting methods 3, 4 and 5.

Low-e coating setting method	U-value ($\text{Wm}^{-2}\text{K}^{-1}$)			
	Emittance: 0.03		Emittance: 0.18	
	Central glazing	Total glazing	Central glazing	Total glazing
Method 3	0.25	0.50	0.56	0.78
Method 4	0.39	0.68	0.64	0.89
Method 5	0.33	0.59	0.60	0.83

Table 7 U-values of the 0.4 m by 0.4 m TVG with emittance of 0.03 and 0.18 in setting methods 6 and 7.

Low-e coating setting method	U-value ($\text{Wm}^{-2}\text{K}^{-1}$)			
	Emittance: 0.03		Emittance: 0.18	
	Central glazing	Total glazing	Central glazing	Total glazing
Method 6	0.54	0.96	0.87	1.22
Method 7	0.38	0.80	0.78	1.12

Figure(s)

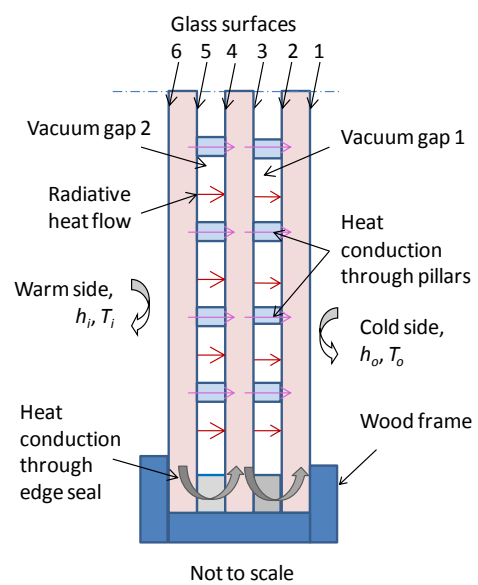


Fig. 1 Schematic diagram of a TVG cross section and heat flow mechanism across the TVG.

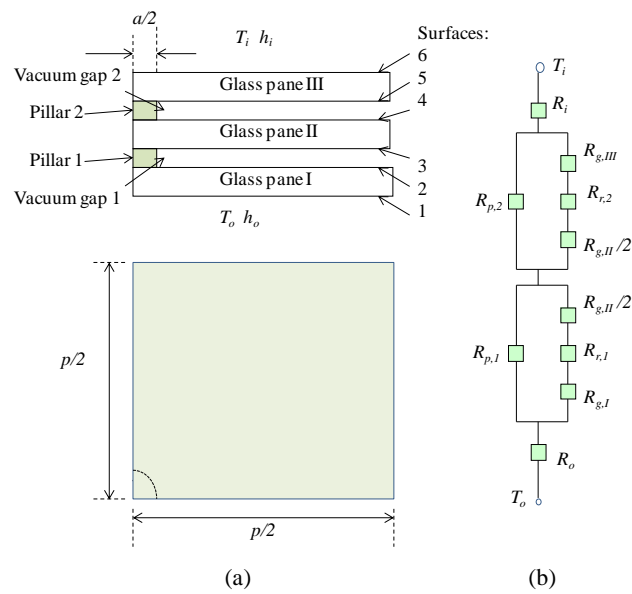


Fig. 2 Schematics of a quarter of a unit cell (a) and its thermal network at the central glazing area (b).

Figure(s)

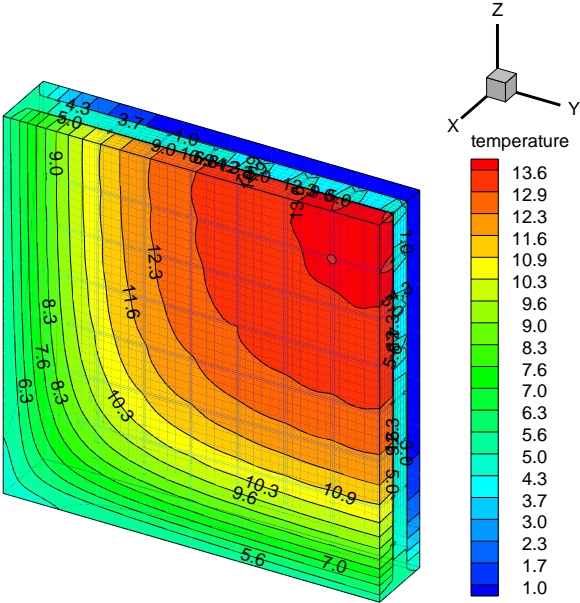


Fig. 3 Isotherms of TVG with four 0.03 emittance low-e coatings.

Figure(s)

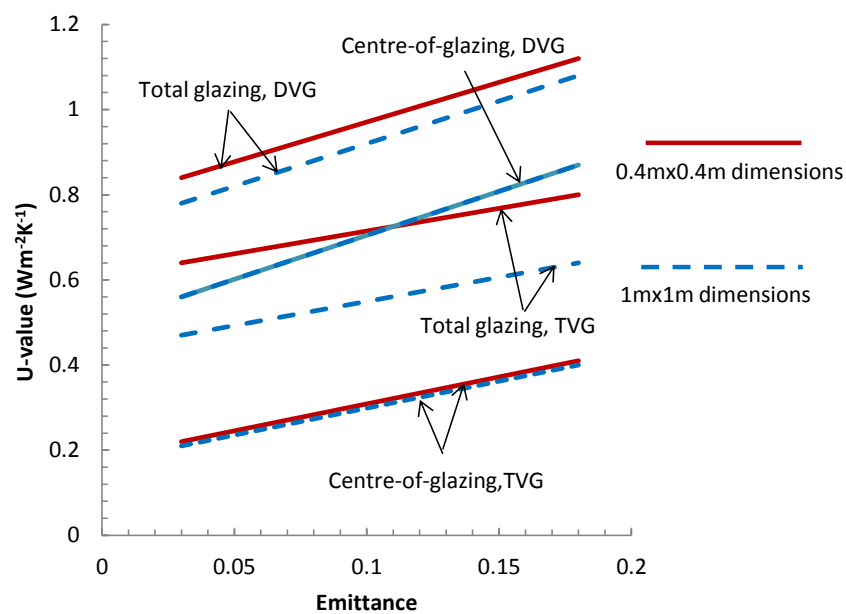


Fig. 4 U-value of the TVGs with four low-e coatings of various emittances.

Figure(s)

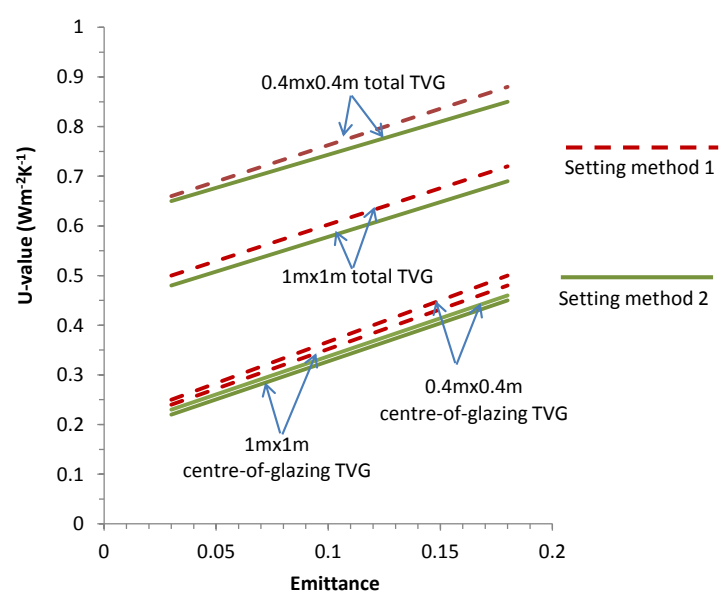


Fig. 5 U-value at centre-of-glazing and total glazing areas of TVGs with three low-e coatings.

Figure(s)

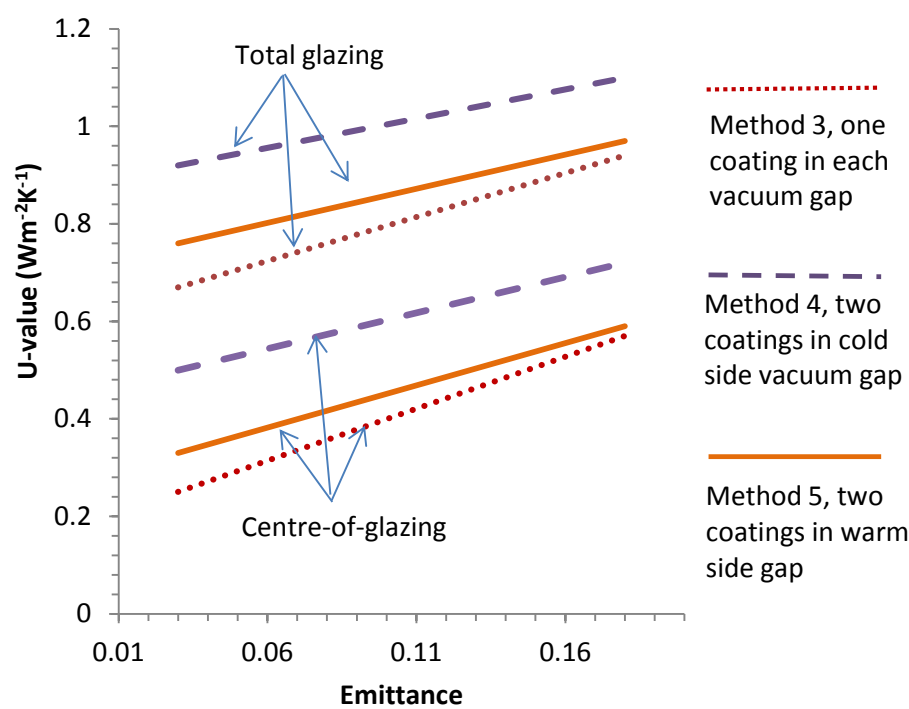


Fig. 6 U-values at the centre-of-glazing and the total glazing areas of the 0.4 m by 0.4 m TVGs with two low-e coatings.

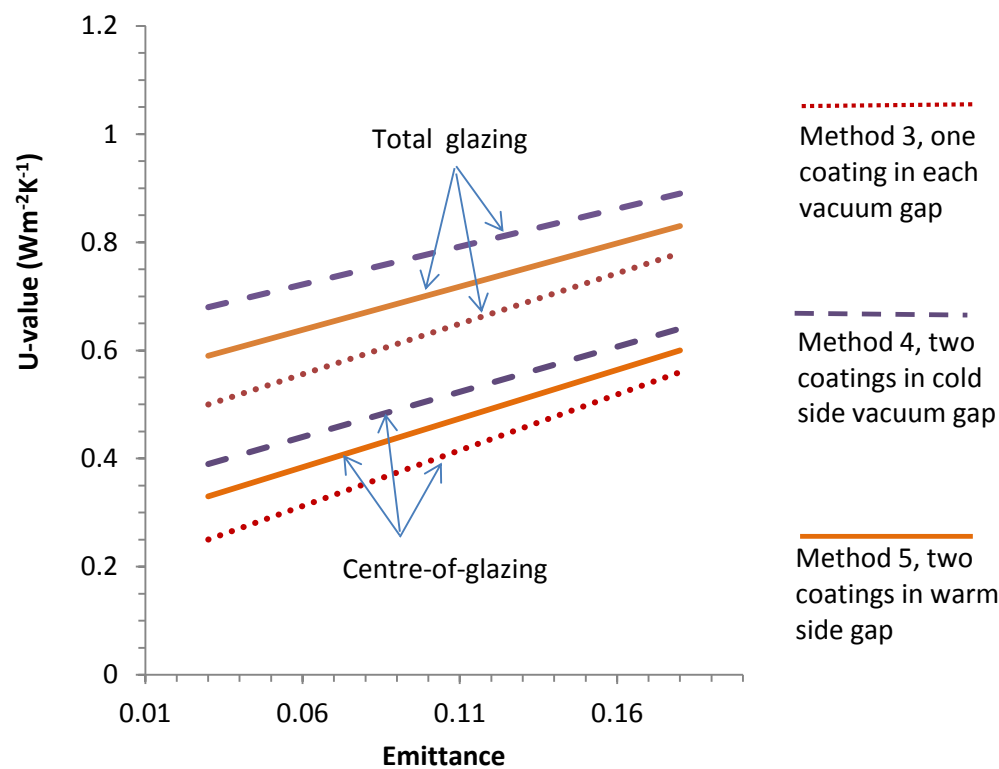


Fig. 7 U-values at the centre-of-glazing and the total glazing areas of the 1 m by 1 m TVGs with two low-e coatings in setting methods 3, 4, 5.

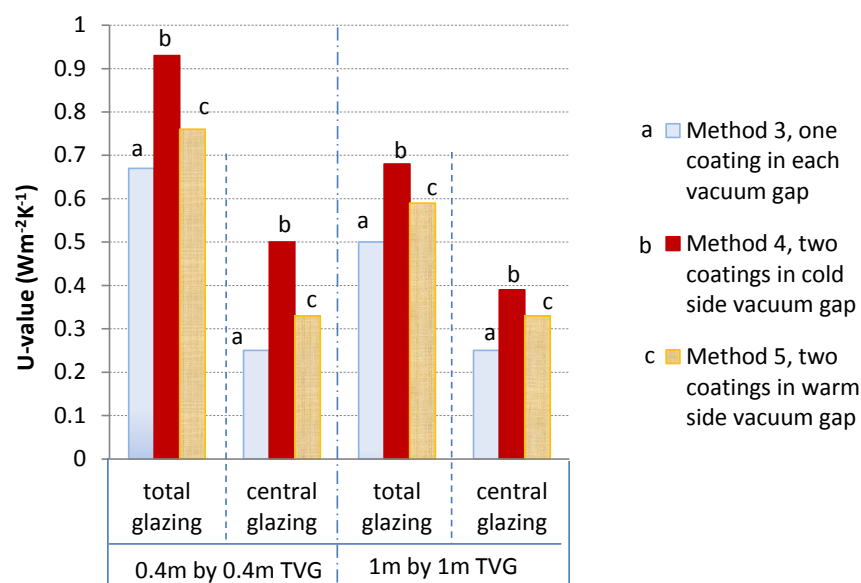


Fig. 8 Comparison of U-value of TVGs with two 0.03 emittance coatings using different setting methods.

Figure(s)

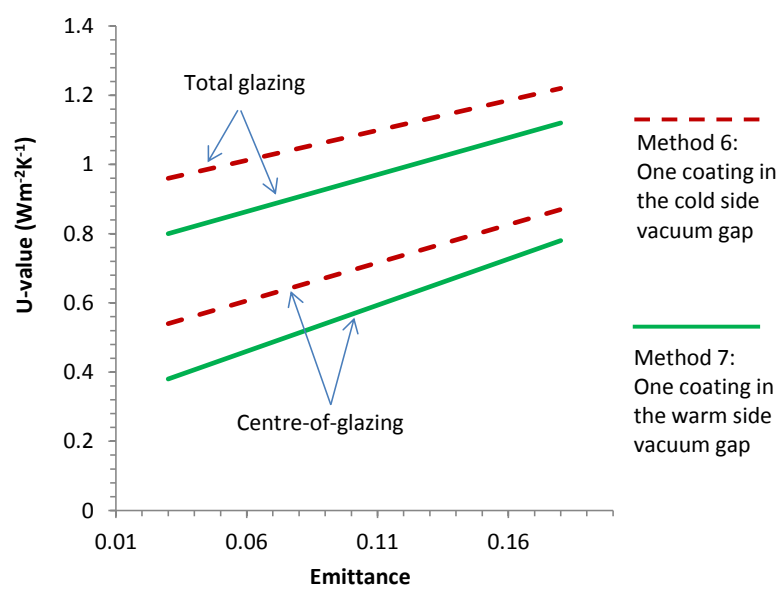


Fig. 9 U-values of 0.4 m by 0.4 m TVGs with one low-e coating in the warm and cold side vacuum gaps.

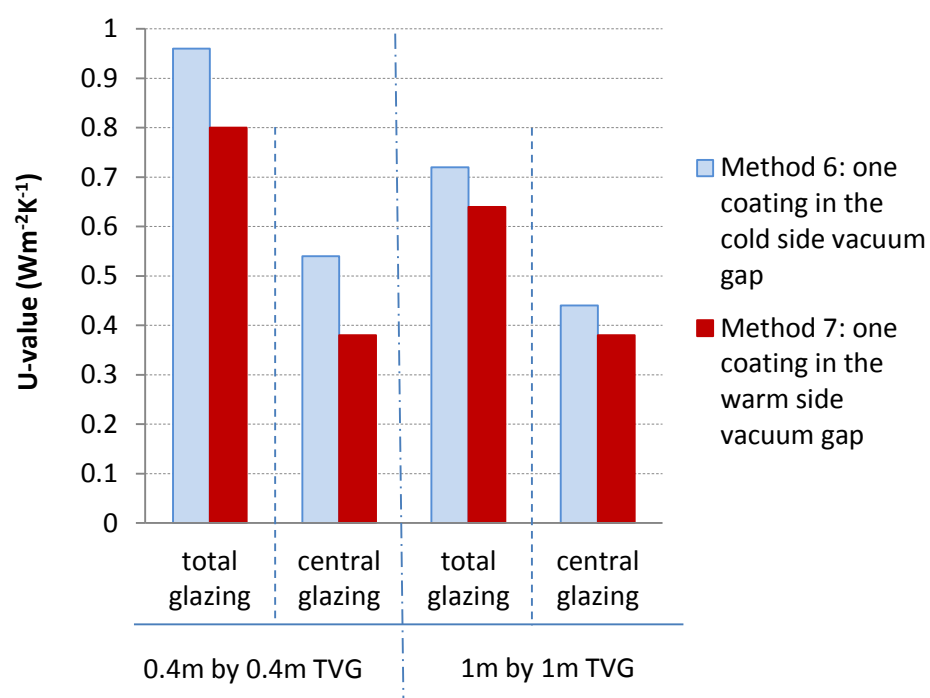


Fig. 10 U-values of TVGs with one 0.03 emittance low-e coating.

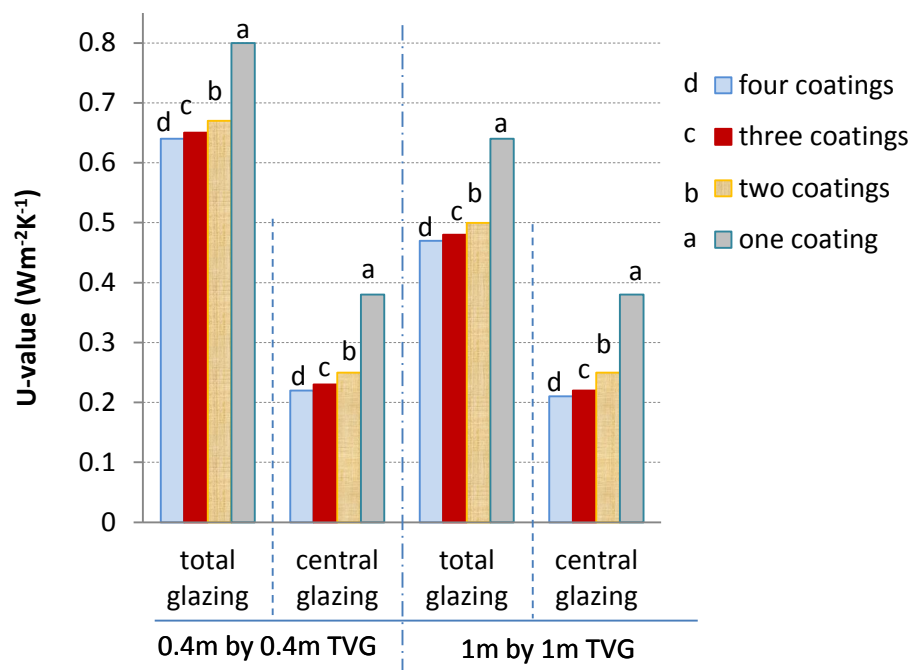


Fig. 11 Comparison of U-values of TVG with one, two, three and four 0.03 emittance coatings.

Figure(s)

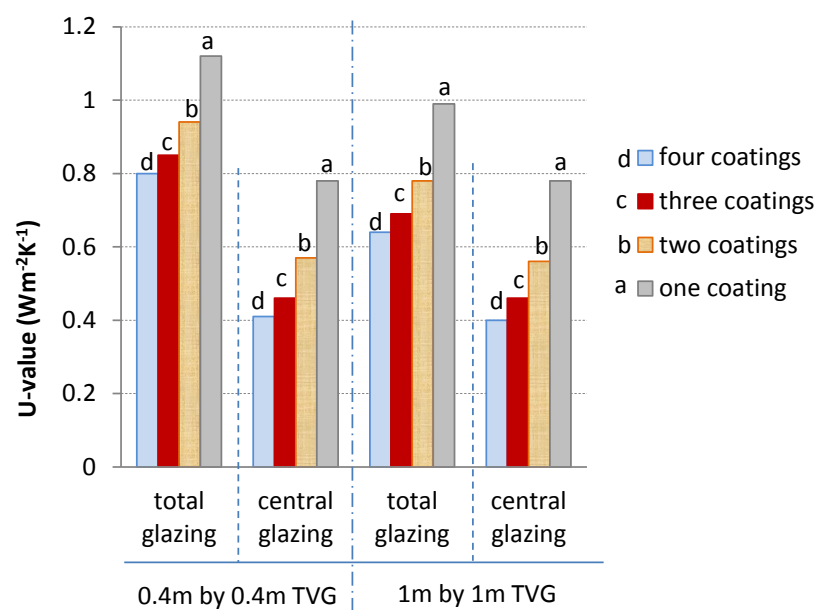


Fig. 12 Comparison of U-values of TVG with one, two, three and four 0.18 emittance coatings.

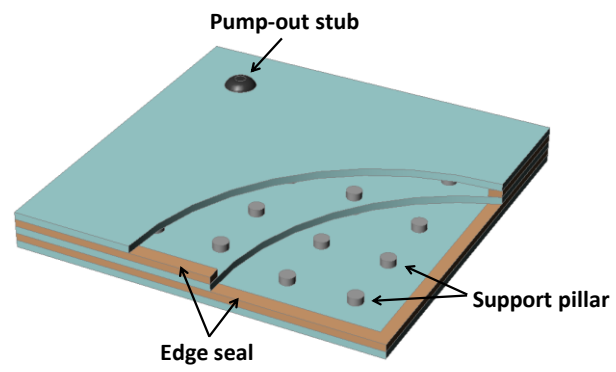


Fig. 13 Schematic diagram of TVG fabricated based using an indium edge seal and pump-out technique.

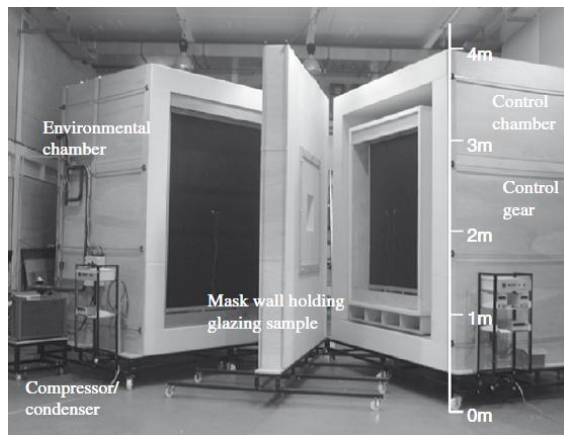


Fig. 14 Guarded hot box calorimeter available at Ulster University.

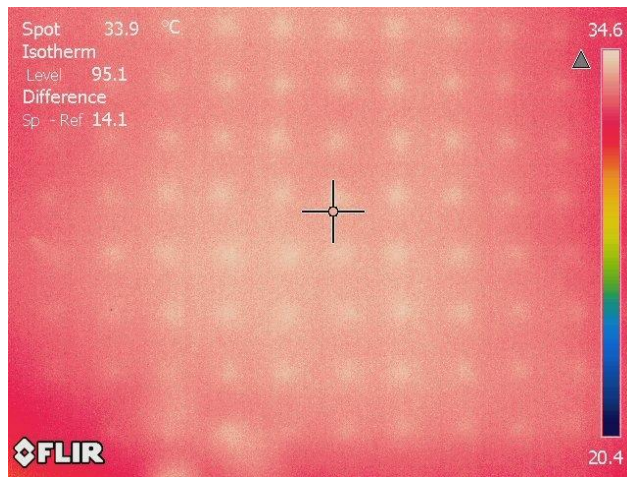


Fig. 15 Isotherms of TVG2 installed within the guarded hot box calorimeter measured using an infrared camera.